VI International Conference on Computational Methods in Marine Engineering
MARINE 2015
F. Salvatore, R. Broglia and R. Muscari (Eds)

TIME DOMAIN SIMULATION OF DYNAMIC POSITIONING MANOEUVRES BASED ON IMPULSE RESPONSE FUNCTIONS

OLE DETLEFSEN*, LASSE THEILEN AND MOUSTAFA ABDEL-MAKSOUD

*Institute for Fluid Dynamics and Ship Theory
Hamburg University of Technology
Am Schwarzenberg Campus 4, 21073 Hamburg, Germany
e-mail: ole.detlefsen@tuhh.de, web page: http://www.tuhh.de/fds

Key words: Seakeeping, Time Domain, Dynamic Positioning

Abstract. The Paper focusses on the development of a numerical method to simulate ship motions under arbitrary external forces. Based on impulse response functions, the developed method benefits from the computational efficiency of boundary element methods in frequency domain to determine hydrodynamic forces acting on the vessel. Major nonlinear effects are captured directly in time domain. To capture the vessels drift motion, second-order wave excitation is considered. Wind and current induced forces complete the modelling of environmental loads. An interface to MATLAB/SIMULINK simplifies an efficient representation of the vessels control system and the dynamics of its propulsion plant. This finally allows time-domain simulations of complex dynamic positioning manoeuvres in natural seaways

1 INTRODUCTION

Up to now, the dynamic positioning capability of ships is mainly judged by balancing available thrust against wind, current and wave induced loads at different encounter angles and sea states. If for a given environmental specification a static equilibrium condition is achieved, the vessel is considered to be able to maintain position. This static procedure neglects several important effects, originating on the one hand from unsteady environmental forces and on the other hand from dynamic interaction between the individual components of the dynamic positioning system itself. In reality, this can lead either to insufficient dynamic positioning performance or high fuel consumption. In contrast, it seems more reasonable to assess the dynamic positioning capability from unsteady seakeeping simulations including the dynamics of the vessels control system and its propulsion plant. Therefore, an efficient method to simulate ship motions in natural seaways under arbitrary external forces in time domain has been developed.

2 IMPULSE RESPONSE FUNCTIONS

The governing equation used for time domain simulations based on impulse response functions was formulated by Cummins [1] already in 1962:

$$(\mathbf{M}+\mathbf{A})\ddot{\vec{\xi}}+\int_0^\infty \mathbf{B}(\tau)\dot{\vec{\xi}}(t-\tau)d\tau+\mathbf{S}\vec{\xi}(t)=\vec{F}(t) \tag{1}$$

In the so-called Cummins Equation, Eqn.(1), $\vec{\xi}$ states a ship motion vector in all six degrees of freedom arising from an arbitrary time domain load $\vec{F}(t)$. $\mathbf{M}$ and $\mathbf{A}$ are the ship's inertia and hydrodynamic mass matrices. Damping forces and fluid-memory effects are modeled by the convolution integral. $\mathbf{S}$ states a linear coefficent matrix for restoring forces and moments. In 1964, Ogilvie [2] shows that instead of solving the non-steady flow potential around the hull directly in each timestep to determine the hydodynamic forces acting on the ship, one can derive the added mass and damping coefficent matrices from more efficient freqency domain based calculations. By comparing the equation of a harmonic ship motion in time domain with its equivalent formulation in frequency domain, Ogilvie states the following relationship for the hydrodynamic mass in time and frequency domain:

$$\mathbf{A}=\mathbf{a}(\omega)+\frac{1}{\omega}\int_0^\infty \mathbf{B}(\tau)\sin(\omega\tau)d\tau \tag{2}$$

Equation(2) obviously holds for any frequency. For an infinite frequency, the second part of the expression is vanishing, which leads to the hydrodynamic mass in time domain as:

$$\mathbf{A}=\mathbf{a}(\omega=\infty) \tag{3}$$

From the comparison of coefficients follows analogously for the hydrodynamic damping:

$$\mathbf{B}(\tau)=\frac{2}{\pi}\int_0^\infty \mathbf{b}(\omega)\cos(\omega\tau)d\omega \tag{4}$$

The hydrodynamic damping coefficents in time domain can then be obtained from inverse fourier transformation of the freqency dependent hydrodynamic damping matrices in Eqn. (4). To determine the hydrodynamic mass and damping in frequency domain, a two dimensional boundary element method [3] is applied. Figure 1 shows the hydrodynamic mass and damping for a wide frequency range. For high frequencies the hydrodynamic mass converges to a constant value, therefore it seems reasonable to evaluate the added mass at a high frequency to fullfill Eqn. (3). The corresponding hydrodynamic damping in time domain, the so-called retardation force, meaning the time decreasing damping force due to a single impulse is plotted on the right.

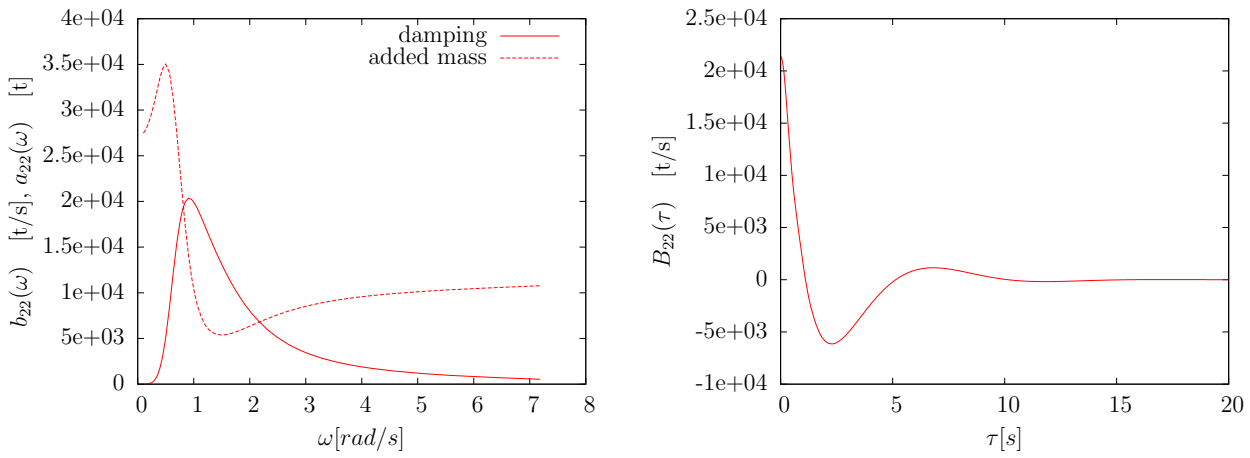

Figure 1: Frequency dependent hydrodynamic mass and damping of pure sway motion for the S-175 containership (left) and retardation function for pure sway motion (right)

3 NUMERICAL SIMULATION METHOD

Within the numerical simulation, the following equation of motion is solved:

$$(\mathbf{M}+\mathbf{A})\,\ddot{\vec{\xi}}(t)+\vec{F}_{\mathbf{B}}(\dot{\vec{\xi}},t)+\vec{F}_{Q}(\dot{\vec{\xi}})+\vec{S}(\vec{\xi},t)=\vec{F}^{(1)}_{Wave}(t)+\vec{F}^{(2)}_{Wave}(t)+\vec{F}_{Ext}(t) \tag{5}$$

Herein, $\mathbf{M}$ is again the matrix of the ship's inertia, where $\mathbf{A}$ is the hydrodynamic mass matrix according to Eqn.(3) and $\vec{\xi}$ is the ship motion vector respective its time derivatives:

$$\vec{\xi}=\begin{pmatrix}\xi_0 & \eta_0 & \zeta_0 & \varphi & \vartheta & \psi\end{pmatrix} \tag{6}$$

$\vec{F}_{\mathbf{B}}(\dot{\vec{\xi}},t)$ states the non-steady retardation forces vector arising from the convolution integral in Eqn.(1):

$$\vec{F}_{\mathbf{B}}(\dot{\vec{\xi}},t)=\int_0^\infty \mathbf{B}(\tau)\dot{\vec{\xi}}(t-\tau)d\tau \tag{7}$$

$\vec{F}_Q$ is a six component vector representing quadratic damping force contributions caused by cross-flow-drag phenomena, viscous surge and roll damping:

$$\vec{F}_Q(\dot{\vec{\xi}})=\vec{F}_q(\dot{\vec{\xi}})+\begin{pmatrix}F_\xi(\dot{\xi}_0) & 0 & 0 & M_\varphi(\dot{\varphi}) & 0 & 0\end{pmatrix}^T \tag{8}$$

Especially for slow-speed-manoeuvring cross-flow-drag is the dominating damping effect and can not be neglected [4]. Therefor a simple two dimensional approach is used here [4,5]. Considering the transverse flow at one section of the ship a sectional damping force

vector $\vec{f}_x(\dot{\vec{\xi}})$ can be calculated as:

$$\vec{f}_x(\dot{\vec{\xi}}) = -\frac{1}{2}\rho \begin{bmatrix} 1 & 0 \\ 0 & 1 \\ z_D & y_D \end{bmatrix} \begin{pmatrix} T(x)C_{Dy}u_{y,x}(\dot{\vec{\xi}})|u_{y,x}(\dot{\vec{\xi}})| \\ B(x)C_{Dz}u_{z,x}(\dot{\vec{\xi}})|u_{z,x}(\dot{\vec{\xi}})| \end{pmatrix} \tag{9}$$

Herein $u_{y,x}(\dot{\vec{\xi}})$ and $u_{z,x}(\dot{\vec{\xi}})$ are the relative velocities in the section plane depending on the ship motion velocity $\dot{\vec{\xi}}$. $T(x)$ is the draft of the section, $B(x)$ its breadth. C_{Dy} and C_{Dz} are numerically or experimentally determined cross-flow-drag coefficients. A common used estimation is $C_{Dy} = 0.8...1.2$ (depending on bilge sharpness) and $C_{Dz} = 0.6$ [3]. The integration over the ship's length then yields to the global damping force:

$$\vec{F}_q(\dot{\vec{\xi}}) = \int_L \mathbf{V}(x)\vec{f}_x(\dot{\vec{\xi}})dx \tag{10}$$

The matrix $\mathbf{V}$ transforms sectional forces into global ship fixed forces. In longitudinal direction also a quadratic damping approach is introduced [6]:

$$F_\xi(\dot{\xi}_0) = -\frac{1}{2}\rho S(1+k_f)C_f(\dot{\xi}_0)|\dot{\xi}_0|\dot{\xi}_0 \tag{11}$$

S is the wetted hull area. k_f is a viscous form factor and $C_f(\dot{\xi}_0)$ a modified friction drag coefficient according to Fossen [6]. A quadratic roll damping moment is stated as in [7]:

$$M_\varphi(\dot{\varphi}) = (d_L + d_Q|\dot{\varphi}|)\dot{\varphi} \tag{12}$$

Herein, d_L and d_Q are linear and quadratic roll damping coefficents which have to be determined externally, for example using model tests or CFD calculations.

$\vec{S}(\vec{\xi}, t)$ are time-dependent nonlinear restoring forces. Based on a sectional approach, the submerged volume and its center of bouyancy is determined in every timestep, according to the actual heel, trim and sinkage of the ship as well as the instantenous wetted surface due to the incident waves. This leads directly to the restoring forces and moments.

$\vec{F}^{(1)}_{Wave}(t)$ and $\vec{F}^{(2)}_{Wave}(t)$ are first respective second order wave excitation forces and moments. As natural seaways are modelled through superposition of regular waves, the first order wave excitation can be calculated also from the superposition of the excitation forces of each wave component [7]:

$$\vec{F}^{(1)}_{Wave}(t) = \sum_{j=1}^{N} \mathrm{Re}\left[\left(\hat{\vec{F}}_{FK}(\omega_j) + \hat{\vec{F}}_{DF}(\omega_j)\right)\hat{\zeta}_j e^{i\omega_{e,j}t}\right] \tag{13}$$

Herein, $\vec{F}_{FK}(\omega_j)$ and $\vec{F}_{DF}(\omega_j)$ state Froude-Krilov respective diffraction force and moment contributions of the j-th wave component. As first order wave excitation alone does not

cause any drift motion of the vessel, it is necessary for DP-related simulations to consider also nonlinear wave excitation. Even though the applied frequency domain boundary element method is just from first order, it allows sufficient information to determine mean second order wave drift forces and moments. The time-averaged mean longitudinal wave drift force for a regular wave can be estimated from first order frequency domain results as follows [3]:

$$\bar{F}_{\xi}^{(2)} = \frac{1}{2}\Bigg(m\omega_e^2 \mathrm{Re}\left(\hat{Y}_{2s}\hat{Y}_6^* - \hat{Y}_{3s}\hat{Y}_5^*\right) + \frac{1}{2}\rho g \sum_{Stb,Port} \int_L |\hat{Y}_z r|^2 \frac{dy_W^+}{dx} dx \\ + \frac{1}{2}\rho g \left(|\hat{Y}_4|^2 - |\hat{Y}_5|^2\right) \left[A_{x0}\left(T + z_{x0}\right)\right]_{\mathrm{transom}} \Bigg) \zeta_a^2 \tag{14}$$

The first term in Eqn. 14 is caused by the ship motion itself, while the second term results from the change in buoyancy due to relative motion alongside the waterline of the ship. A correction for flow separation at an immersed transom at higher forward speeds is introduced by the last term, it can be neglected in case of slow-speed manoeuvring. The time-averaged mean transverse drift force is derived accordingly [3]:

$$\bar{F}_{\eta}^{(2)} = \frac{1}{2}\left(\rho g \sum_{Stb,Port} \int_L y_W^+ \mathrm{Re}\left(\hat{Y}_{z_{r0}} \hat{Y}_{\zeta_{Wy}}\right) dx - m\omega_e^2 \mathrm{Re}\left(\hat{Y}_{1s}\hat{Y}_6^*\right) \right) \zeta_a^2 \tag{15}$$

According to Söding [8], a time-averaged yaw drift moment can be derived as:

$$\bar{M}_{\zeta}^{(2)} = -\frac{1}{2}\omega_e^2 \mathrm{Re}\left[\hat{\vec{\alpha}}^* \times \Theta \hat{\vec{\alpha}}\right]_{\zeta} + \sum_{WL-Panels} \left((\vec{\underline{x}} - \vec{\underline{x}}_G) \times \left[\frac{|\hat{p}_w|^2}{4\rho g} \vec{\Delta s}(0,0,-1) \right] \right)_{\zeta} \\ + x_G \bar{F}_{\eta}^{(2)} - y_G \bar{F}_{\xi}^{(2)} \tag{16}$$

Herein, the first component results from rotational ship motions. The next term follows from the integrated second order wave pressure over the wetted hull surface. Finally, the yaw moment originating from longitudinal and transverse drift force is added in the last term. From the time-averaged mean values a time series of drift forces and moments can be generated again. Therefor, a simple but reasonable approach [9] derived from statistical description of natural seaways is used. Assuming that the second order drift forces and yaw moment are varying with the square of the seaway envelope $a^2(t)$, one obtains a time domain drift force as [9]:

$$F^{(2)}(t) = \frac{1}{2}\rho g L\, \alpha_0^2\, a^2(t) \tag{17}$$

The significant drift force coefficient α_0^2 for a given seaway can be calculated as the weighted mean average of the wave components drift forces according to their energy

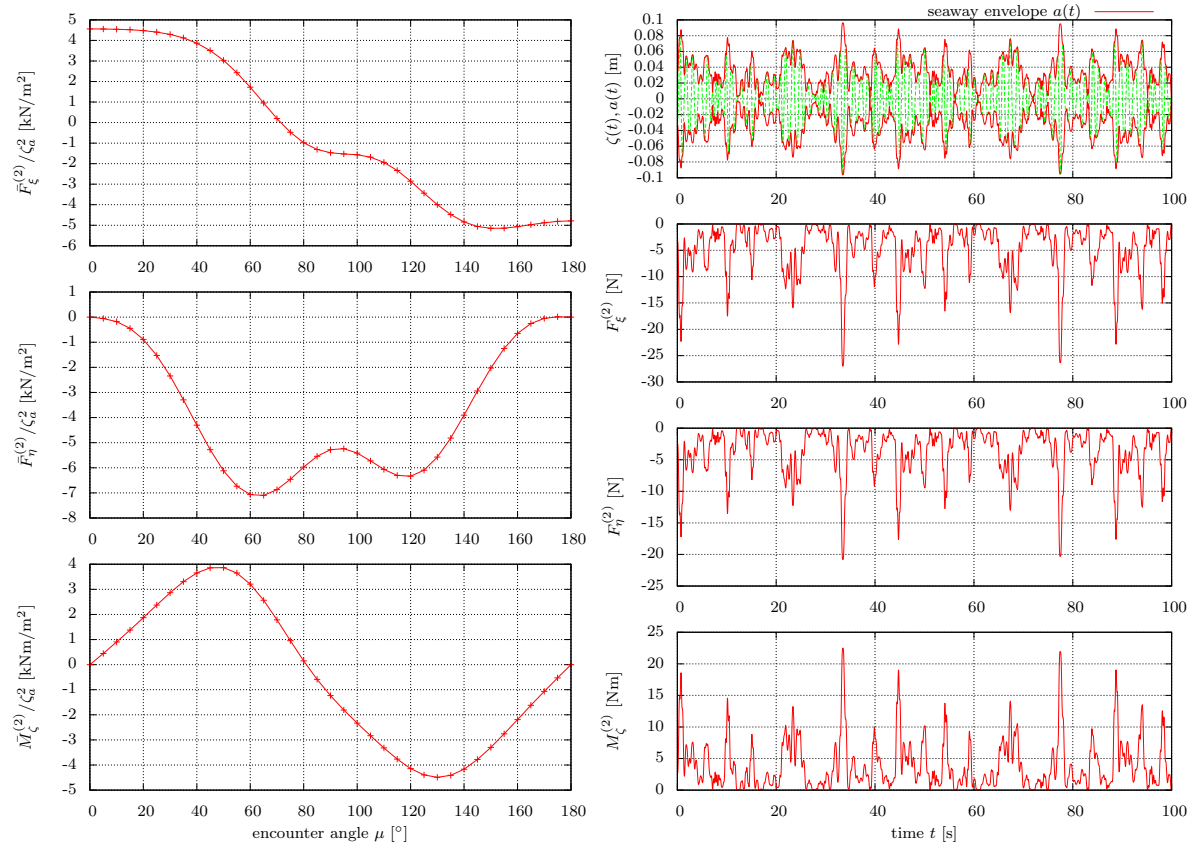

Figure 2: Significant drift forces and yaw moment vs. encounter angle(left), generated time domain drift forces and yaw moment (right)

contribution to the whole seaway:

$$\alpha_0^2 = \frac{\int_0^\infty \alpha^2(\omega) S_\zeta(\omega) d\omega}{\int_0^\infty S_\zeta(\omega) d\omega} \tag{18}$$

Herein, $S_\zeta(\omega)$ states the energy density spectrum of the seaway, whereas $\alpha^2(\omega)$ is a nondimensional drift force coefficient of a wave component:

$$\alpha^2(\omega) = \frac{F^{(2)}(\omega)}{\frac{1}{2}\rho g L \zeta_a^2(\omega)} \tag{19}$$

Using the significant wave frequency $\omega_0 = 2\pi/T_0$ of the seaway, the seaway envelope then follows as:

$$a^2(t) = \zeta^2(t) + \frac{\left(\frac{d\zeta}{dt}\right)^2}{\omega_0^2} \tag{20}$$

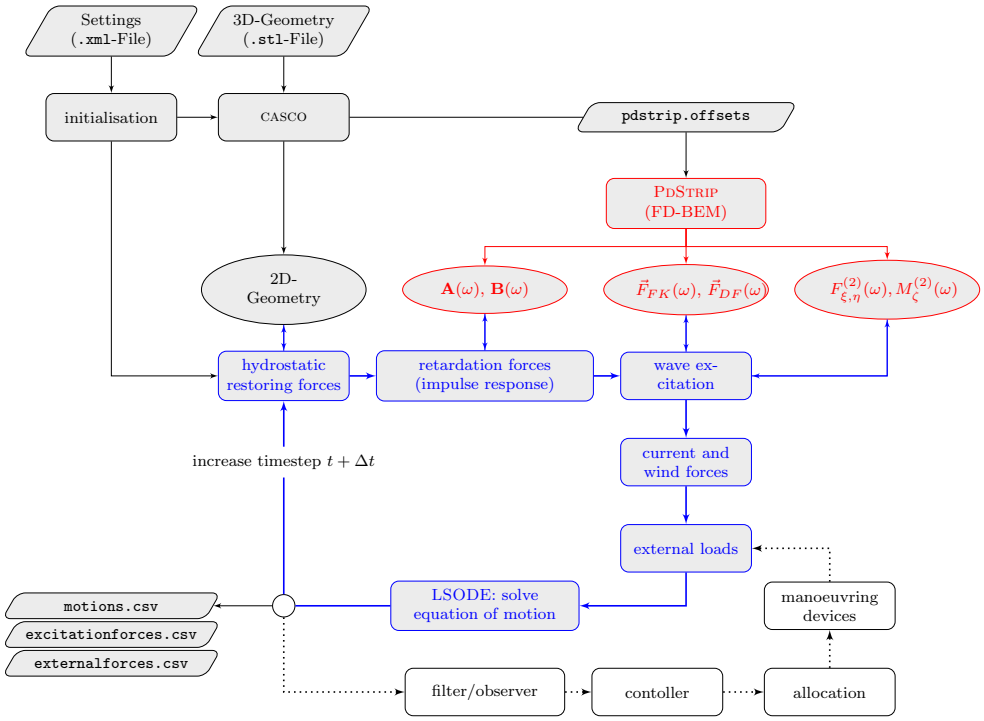

Figure 3: Flowchart of the numerical method and possible coupling to a DP system

Figure 2 shows examplarily mean longitudinal and transverse drift forces and the yaw drift moment depending on the wave encounter angle. On the right a corresponding time domain drift force signal is shown. One observes that the generated drift force signals are following the seaway envelope.

$\vec{F}_{Ext}(t)$ is a six component vector allowing the consideration of arbitrary external forces and moments.

The numerical method is implemented in Fortran. Figure 3 shows the flowchart of the simulation method. As input, a three dimensional surface descripton of the hull geometry is needed. A .xml-file is used to define the simulation settings, e.g. the vessel's load-case, seaway settings or damping coefficients. Within the initialisation, two dimensional sections are generated from the hull geometry. Then PdStrip [3], a two dimensional boundary element method (strip method) is applied to compute the hydrodynamic mass and damping and the wave excitation forces in frequency domain. A second sectional geometry is created, including all watertight compartments of the vessel which contribute to hydrostatic restoring forces. The hydrostatic restoring forces and moments are calculated at the beginning of each timestep. Then the retardation forces are evaluated and viscous damping contributions are added. After the wave excitation forces have been determined, the external forces are taken into account, e.g. wind and current loads or forces arising from thrusters or other manouevring devices. The equation of motion is then solved using a fourth order Runge-Kutta integration scheme and the simulation proceeds with the next

timestep. To simplify the modelling of further external forces and to allow an easy representation of vessel control and allocation systems for dynamic positioning simulations, the simulation method has been cast into the MATLAB-MEX API. Major simulation routines then can be called directly from MATLAB or SIMULINK and are handled like built-in functions.

4 VALIDATION

The developed simulation method has been validated with the results of a model tests conducted at the Potsdam Model Basin. For the seakeeping tests, a tug model equipped with two Voith Schneider propellers was used. The ship motions have been measured in several regular and irregular waves at zero speed. To allow a direct comparision of measured and calculated motions, the wave train used in the model test tank was decomposed into 200 wave components using fourier transformation. The same wave components have then been used as input for the simulations. Figure 4 shows exemplarily the comparison between tank test and simulation results in irregular waves at an encounter angle of $\mu = 180°$. The motions show reasonable agreement, especially phase and frequency of the motion are matching very well. It seems that the damping used in the simulation is less than in the model test. During the seakeeping tests, the tug model was secured with lines, which causes the visible low frequency motion in the model test. Other encounter angles show the same good agreement of simulated and measured motions [5].

5 APPLICATION TO DYNAMIC POSITIONING

5.1 Modelling of wind and current induced loads

To complete the modelling of environmental loads, wind and current forces are considered. To capture the wind speed fluctuations, a dynamic wind model according to Blendermann is used [10]. From a statistical analysis of the wind speed fluctuation the following non dimensional wind gust spectrum according to Davenport can be stated [10]:

$$\frac{f S_{Gust}(f)}{C_{10}\bar{u}_{10}^2} = \frac{1}{\left[1 + \left(\frac{L_{oa}}{L}\right)^{4/3} \tilde{f}^{4/3}\right]^2} \frac{4}{\left(1 + \tilde{f}\right)^{4/3}}, \qquad \tilde{f} = \frac{fL}{\bar{u}_{10}} \tag{21}$$

Like the superposition of regular waves to represent natural seaways, the superposition of wind gusts leads to a non-steady wind signal [10]:

$$u_w(t) = \bar{u}_{10} + \sum_{i=1}^{n} \sqrt{2 S_{Gust}(f_i) \Delta f_i} \cos(2\pi f_i t + \varphi_i) \tag{22}$$

Figure 5 shows a typical Davenport wind gust spectrum and a corresponding time domain wind signal. A common way to calculate wind loads for given wind speeds u_w and angles of attack ε is the usage of experimentally or numerically determined non-dimensional wind

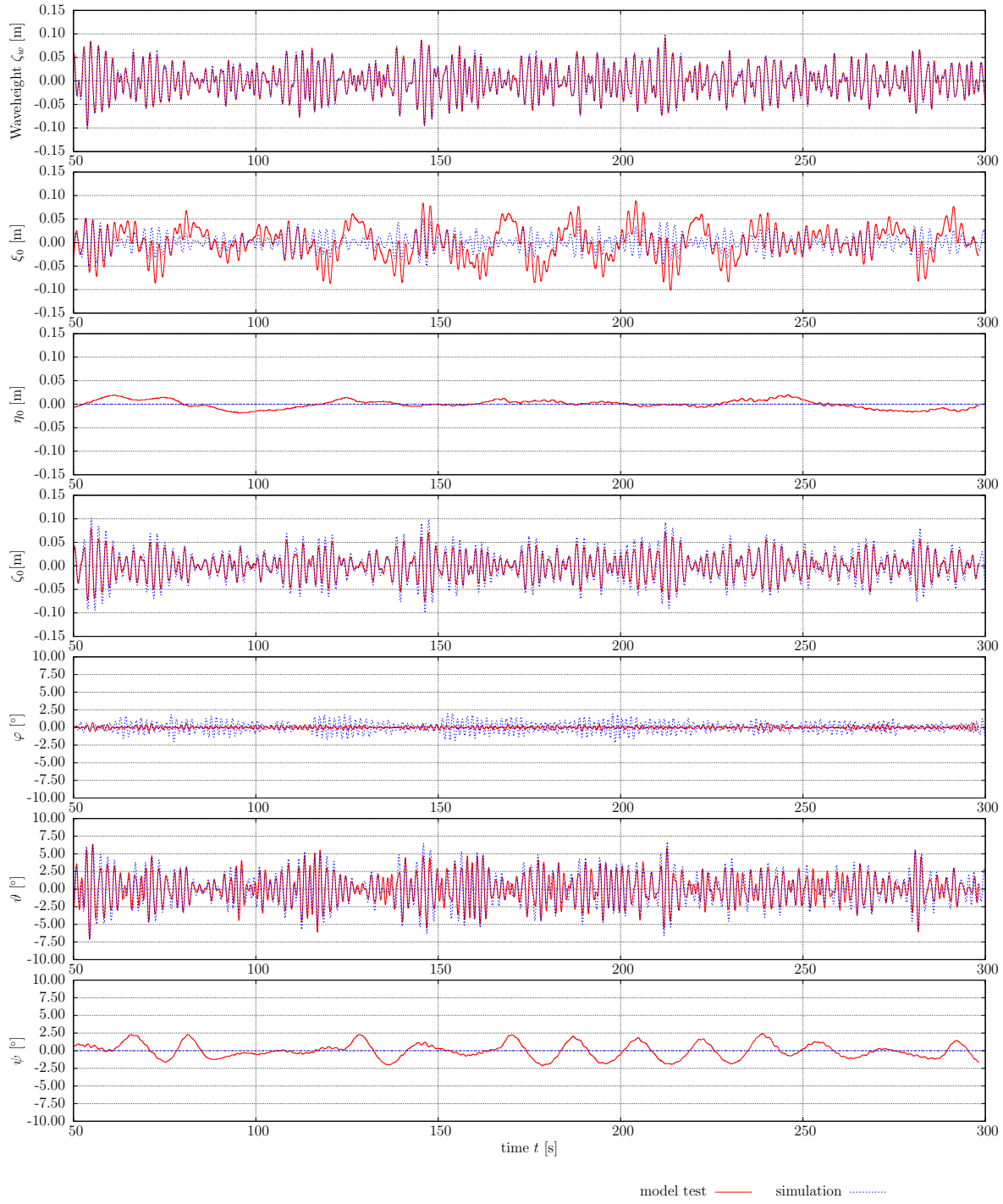

Figure 4: Comparison between ship motions in irregular waves obtained by model test and simulation

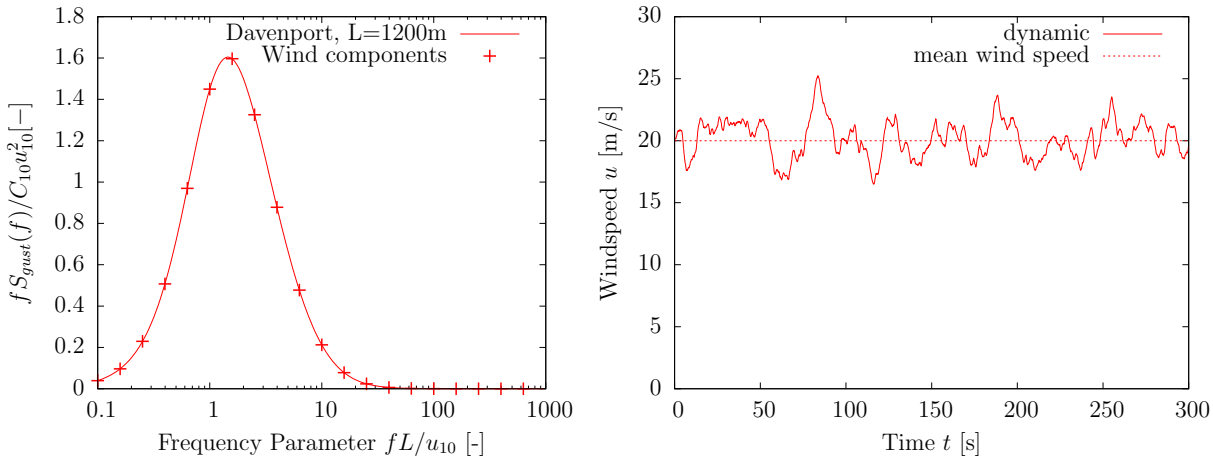

Figure 5: Davenport Wind Spectrum and generated time domain wind speed fluctuation

load coefficients [10]:

$$\vec{F}_{Wind}(t) = \begin{pmatrix} C_X(\varepsilon) & C_Y(\varepsilon) & 0 & C_K(\varepsilon)\bar{H} & 0 & C_N(\varepsilon)L_{oa} \end{pmatrix}^T \frac{\rho_{air}}{2} u_a(t)^2 A_L \tag{23}$$

In case of vanishing or small ship speed like at DP operations, the apparent wind speed u_a equals the true wind speed u_w. A_L is the lateral plane area, where L_{oa} is considered to be the reference length and $\bar{H}$ the mean height of the lateral plane.

For current induced loads, a static approach seems reasonable enough, because current speed variations, e.g. caused by tidal flow, occur at very low frequencies. As for the wind loads, a coefficient based approach [11] is used again to compute current induced forces and moments for a static current speed u_c:

$$\vec{F}_{Current}(t) = \begin{pmatrix} C_{X,c}(\varepsilon)B & C_{Y,c}(\varepsilon)L_{oa} & 0 & 0 & 0 & C_{N,c}(\varepsilon)L_{oa}^2 \end{pmatrix}^T \frac{\rho}{2} u_c^2 T \tag{24}$$

$C_{X,c}$,$C_{Y,c}$ and $C_{N,c}$ are externally determined current load coefficients, while B and T are the vessel's breadth and draft.

The wind and current induced forces and moments are then considered in the simulation using the external forces interface:

$$\vec{F}_{Ext}(t) = \vec{F}_{Wind}(t) + \vec{F}_{Current}(t) \tag{25}$$

5.2 Representation of the DP system

For an easy representation of the vessels DP system, the simulation method has been integrated into a SIMULINK model. To determine the required longitudinal and transverse forces and the yaw moment to hold position, a nonlinear PID controller is used. Within the allocation module the thrust is distributed between the two Voith-Schneider units,

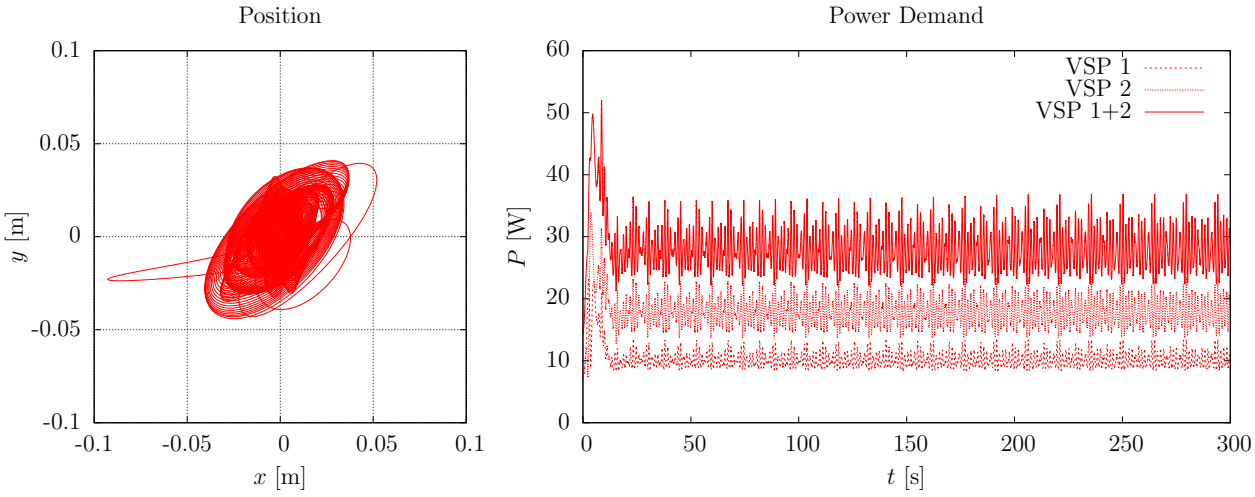

Figure 6: A DP-simulation with the tug model: Position of the vessel (left) and power demand of the Voith Schneider propulsion units (right)

taking into account the dynamics of the propulsion train. Because only the drift motion of the vessel should be compensated, a Kalman filter is used to seperate the wave frequency contributions from the ship motion.

Figure 6 shows the results of a DP simulation for the tug model. The tug model is exposed to short crested waves at an encounter angle of $\mu = 135°$ with $T_0 = 1.225$s and $H_{1,3} = 0.2$m. The mean wind speed is set to $\bar{u}_{10} = 2.0$m/s at the same angle of attack. Current is assumed with $u_c = 0.4$m/s in the same direction. The Figure shows the position of the vessel during the manoeuvre and the power demand of the Voith Schneider propellers. In the examined case, the deviation from the desired position at $(0, 0)$ is remarkable small, which is caused in the fast reaction capacity of the Voith Schneider propellers.

6 CONCLUSION AND OUTLOOK

The paper outlines the development of a robust and efficient numerical method to simulate ship motions in seaways under the consideration of arbitrary external loads. Based on impulse response functions, the developed method benefits from the computational efficiency of boundary element methods in frequency domain to determine hydrodynamic mass and damping forces, whereas important nonlinear force components are treated directly in time domain. The method is currently validated. First comparisons with model test results of a tug boat show good agreement. For the application to dynamic positioning related problems, the simulation method has been extended to capture wave drift forces and loads arising from wind and current. To allow an easy integration of control systems, an interface to MATLAB has been implemented. The simulation method is currently used to investigate different dynamic positioning configurations and to optimize their control

and allocation systems. After conducting hardware-in-the-loop tests with the later on board installed automation system hardware, wherefore the simulation method is also used, final model tests with full equipped and actuated models are planned. In the near future the strip method is replaced with three dimensional boundary element methods to obtain hydrodynamic force coefficients. This can result in a further increase of accuracy, especially for more blunt ship shapes, where three dimensional effects are dominating.

7 ACKNOWLEDGEMENT

The present work has been carried out within the research project DPMotion-AuDyPos funded by the Federal Ministy of Economics and Technology of Germany. The authors express their thanks to the project partners at Voith Turbo Schneider Propulsion GmbH & Co. KG in Heidenheim for providing the allocation module, the Institute of Automation of the University of Rostock for designing a first DP controller and the Potsdam Model Basin for conducting model tests.

REFERENCES

[1] Cummins, W. E. *The Impulse Response Function and Ship Motions* (1962).

[2] Ogilvie, T. Recent Progress towards the Understanding and Prediction of Ship Motions, in *Proceedings of the 5th Symposium on Naval Hydromechanics* (1964).

[3] Bertram, V., and Söding, H. *Program PDSTRIP: Public Domain Strip Method*, Manual (2009).

[4] Brix, J. E. *Manoeuvring Technical Manual*, (1992).

[5] Detlefsen, O. *Entwicklung eines Verfahrens zur Simlulation von Schiffsbewegungen und dynamischem Positionieren im Seegang unter Verwendung von Impuls-Antwort-Funktionen*, master's thesis (2014).

[6] Fossen, T. I. *Handbook of Marine Craft Hydrodynamics and Motion Control*, (2011).

[7] Kröger, H.-P. *Simulation der Rollbewegung von Schiffen im Seegang*, IfS-Report No. 473 (1987).

[8] Söding, H. *Berechnung von Driftkräften und -momenten schwimmender Körper in Wellen*, unpublished (2013).

[9] Clauss, G., and Lehmann, E., and Östergaard, C. *Offshore Structures Volume II: Strength and Safety for Structural Design*, (1994).

[10] Blendermann, W. *Practical Ship and Offshore Structure Aerodynamics*, (2011).

[11] Journée, J. M. J. and Massie, W. W. *Offshore Hydromechanics*, (2001).